

Pattern selection and tip perturbations in the Saffman-Taylor problem

D. C. Hong and J. S. Langer

Institute for Theoretical Physics, University of California, Santa Barbara, California 93106

(Received 30 January 1987)

We present an analytic approach to the Saffman-Taylor problem of predicting the width of a viscous finger in a Hele-Shaw cell. Our first purpose is to provide a systematic description of the way in which the singular perturbation introduced by capillary forces leads to a solvability mechanism for pattern selection. We then show how recent experimental observations by Couder *et al.* may be interpreted in terms suggested by this mechanism. In particular, we show that the remarkable changes in pattern selection induced by bubbles trapped at the tips of fingers can be explained by assuming that the perturbation caused by a bubble is effectively equivalent to a positive opening angle at the tip.

I. INTRODUCTION

Our purpose in this paper is, first, to present a relatively simple and systematic description of the solvability theory for pattern selection in the Saffman-Taylor problem¹ and, second, to show how this theory can be used to explain some remarkable experimental observations reported recently by Couder and co-workers.^{2,3}

The Saffman-Taylor problem, that is, the problem of predicting the shape of the fluid finger that forms in a Hele-Shaw cell, is similar in many respects to the problem of predicting the shape and speed of the tip of a dendritic crystal growing in an undercooled melt.⁴ Pattern selection in both of these problems turns out to be controlled by surface tension, an ostensibly small but singular perturbation which converts an equation with a continuous family of steady-state solutions into one for which such solutions exist only for a discrete set of values of some parameter, for example, the finger width or the growth rate. Among those configurations which satisfy such a solvability condition, there generally exists just one which can be identified as the dynamically selected state of the system.

The solvability mechanism in the Saffman-Taylor problem was first discovered in numerical investigations by McClean and Saffman⁵ and by Vanden-Broeck.⁶ Analytic versions of the theory subsequently were presented in short, simultaneous publications by Shraiman,⁷ Combescot *et al.*,⁸ and the present authors.⁹ Although all three of the latter papers reach identical and—we believe—correct conclusions, they are each written from rather different points of view. Our own paper,⁹ we now recognize, is misleading at best; thus we feel a special obligation to provide a clearer and more detailed account of the situation.

The specific approach that we shall adopt here is essentially the same as the one that we used in a recent discussion of the dendrite problem.¹⁰ (See also Pelcé and Pomeau¹¹ and Ben-Amar and Pomeau.¹²) It is closely related to the point of view presented by Shraiman⁷ and depends, for a really deep understanding of its validity, on the nonlinear analysis of Combescot *et al.*⁸ In particular, we derive a linear inhomogeneous integrodifferential equation for capillary corrections to the shape of the Saffman-Taylor finger and, from this, deduce via

Wentzel-Kramers-Brillouin (WKB) methods a necessary condition for the existence of solutions. Section II of this paper should be understood as a reformulation of the Saffman-Taylor problem in terms directly analogous to those used in Ref. 10; the results are the same as those presented in Refs. 7–9. Section III contains our interpretation of Couder's experiments^{2,3} in which he has perturbed the flow in the neighborhood of the tip of the finger by trapping a small bubble at that point. As we shall see, his results appear to be a strong confirmation of the solvability mechanism for pattern selection.

II. SOLVABILITY CONDITION FOR THE SAFFMAN-TAYLOR FINGER

Our starting point is the nonlinear integrodifferential equation originally derived by McClean and Saffman⁵ to compute the shape of the steady-state finger. The system of interest, shown schematically in Fig. 1, is an effectively two-dimensional channel of width $2W$ and thickness $b \ll W$ along which a fluid of viscosity μ is being pushed by an immiscible second fluid of relatively negligible viscosity. Both fluids are incompressible. The steady-state configuration of this system is observed experimentally to be one in which the inviscid pushing fluid forms a

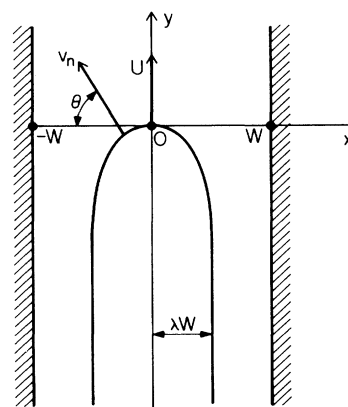


FIG. 1. Schematic diagram of the Saffman-Taylor finger. Note that in our notation the channel has a total width $2W$.

finger of width $2\lambda W$ along the center of the channel; and the problem to be solved is to compute λ as a function of W , b , μ , the speed of the finger U , and the interfacial tension γ . Observations of ordinary fingers—without Couder's perturbations at their tips—indicate that λ is always greater than $\frac{1}{2}$ and that it approaches $\frac{1}{2}$ as a limiting value as U becomes large.

The underlying physical equations of motion for this model are relatively simple. The velocity \mathbf{v} of the viscous fluid is given everywhere by Darcy's law:

$$\mathbf{v} = -\frac{b^2}{12\mu} \nabla p = \nabla \phi, \quad (2.1)$$

where p is the pressure and ϕ is a velocity potential. Incompressibility implies that ϕ satisfies Laplace's equation:

$$\nabla^2 \phi = 0. \quad (2.2)$$

Boundary conditions at the surface of the finger are

$$v_n = \frac{\partial \phi}{\partial n}, \quad (2.3)$$

where v_n is the velocity of the boundary along its outward normal and $\partial/\partial n$ denotes differentiation along this normal, and

$$\phi_s = \frac{b^2 \gamma}{12\mu} \kappa, \quad (2.4)$$

where ϕ_s is the value of ϕ at the surface and κ is the curvature. At the walls of the channel, the viscous fluid is conveniently assumed to obey pure slip boundary conditions. Far behind the tip of the finger, the viscous fluid remains at rest; far ahead of the tip, where this fluid is being expelled from the channel, it must be moving at a uniform speed λU .

Equations (2.2)–(2.4) would be formally identical to the defining equations for the "one-sided" model of solidification⁴ if Laplace's equation (2.2) were replaced by the diffusion equation, that is, if ϕ could be interpreted as a thermal field. Indeed, the two problems are isomorphic to one another in the limit of infinitely fast diffusion or infinitesimally slow motion; but one must be very careful in taking these limits. In the present situation, where ϕ satisfies Laplace's equation and has effectively an infinite range in two dimensions, the motion of the finger is controlled by its interaction with the walls of the channel. This interaction turns out to play a role in the fingering problem that is very similar to the role played by crystal-line anisotropy for the dendrite.

McClellan and Saffman⁵ have used conformal methods to transform this problem into a nonlinear integrodifferential equation for the shape of the steady-state boundary. They specify this boundary by writing θ , its angle of orientation as shown in Fig. 1, as a function of a real variable s . In their notation, $s=1$ at the tip of the finger and $s \rightarrow 0$ infinitely far back along one side; $\theta(1) = -\pi/2$ (at the tip) and $\theta(0) = 0$. Their equation then turns out to be

$$vqs \frac{d}{ds} \left[qs \frac{d\theta}{ds} \right] = q - \cos \theta, \quad (2.5)$$

where the function $q(s)$ is defined by

$$\ln q(s) = -\frac{s}{\pi} \mathbf{P} \int_0^1 ds' \frac{\theta(s')}{s'(s'-s)} \quad (2.6)$$

and

$$v = \frac{b^2 \gamma \pi^2}{12\mu U W^2 (1-\lambda)^2} \quad (2.7)$$

is the (presumably) small dimensionless parameter which contains the surface tension. The function $q(s)$ is proportional to the tangential velocity of the finger or, equivalently, the tangential velocity of the viscous fluid at the boundary of the finger in a frame of reference in which the finger is at rest. Accordingly, $q(0) = 1$ and $q(1) = 0$. The symbol \mathbf{P} in (2.6) denotes the Cauchy principal value. The reader should refer to the original paper of McClellan and Saffman⁵ for a detailed derivation of these results.

When the surface tension vanishes, $v=0$, (2.5) and (2.6) can be solved explicitly to yield¹

$$q_0(s) = \cos \theta_0(s) = \left[\frac{1-s}{1+\alpha s} \right]^{1/2}, \quad (2.8)$$

where $\alpha = (2\lambda - 1)/(1 - \lambda)^2$. In the Cartesian coordinates (x, y) shown in Fig. 1, this solution becomes

$$y = \frac{2(1-\lambda)W}{\pi} \ln \cos \left[\frac{\pi x}{2\lambda W} \right]. \quad (2.9)$$

Note that this solution is valid for any value of the width λ in the physically meaningful range $0 \leq \lambda \leq 1$; thus, in the absence of surface tension, we have a continuous family of solutions and no explanation for the sharp selection of λ that is seen experimentally. There is no hint, at this stage of the analysis, of why the value $\lambda = \frac{1}{2}$ should have some special significance.

Our next step is to let v be small but nonzero and linearize (2.5) and (2.6) in the neighborhood of the solution (2.8). We define

$$\theta(s) = \theta_0(s) + v\theta_1(s), \quad (2.10)$$

and obtain an inhomogeneous linear equation of the form:

$$v \frac{d^2 \theta_1}{ds^2} + vP(s) \frac{d\theta_1}{ds} + Q(s)\theta_1 + H(s)\mathbf{P} \int_0^1 ds' \frac{\theta_1(s')}{(s'-s)} = R(s), \quad (2.11)$$

where

$$P(s) = \frac{1}{s} - \frac{(1+\alpha)}{2(1-s)(1+\alpha s)}, \quad (2.12a)$$

$$Q(s) = \frac{(1+\alpha)^{1/2}(1+\alpha s)^{1/2}}{s^{3/2}(1-s)}, \quad (2.12b)$$

$$R(s) = \frac{(1+\alpha)^{1/2}}{2s^{1/2}(1-s)^{1/2}(1+\alpha s)} \left[\frac{1}{2s} - \frac{3\alpha}{2(1+\alpha s)} \right], \quad (2.12c)$$

$$H(s) = \frac{(1+\alpha s)^{1/2}}{\pi s^2(1-s)^{1/2}}. \quad (2.12d)$$

Relevant boundary conditions are $\theta_1(0)=\theta_1(1)=0$. If we set $\nu=0$ in (2.11), the remaining equation is identical to Eq. (29) of McClean and Saffman; that is, the solution of the remaining inhomogeneous integral equation would be the first term in a regular perturbation expansion for $\theta(s)$ in powers of ν .

We have departed from McClean and Saffman at this point in that we have retained two terms in (2.11) that contain explicit factors ν and which, therefore, appear to be of higher order in this small parameter. Our reason for keeping these particular terms is that they contain derivatives of θ_1 with respect to s , which means that they are singular perturbations which cannot necessarily be discarded without missing essential features of the problem. Other nonsingular terms proportional to ν in (2.11) have, in fact, been omitted.

Before going on to a detailed discussion of the role played by this singular perturbation, we find it convenient to replace s in Eqs. (2.11) and (2.12) by the independent variable η :

$$\eta = -\cot\theta_0(s) = \left[\frac{1-s}{(1+\alpha)s} \right]^{1/2}. \quad (2.13)$$

In terms of the Cartesian coordinates shown in Fig. 1, η is the slope dy/dx which may be taken to vary from $-\infty$ to $+\infty$ as one goes all the way around the finger from the right-hand side to the left, passing through $\eta=0$ at the tip. We also find it convenient at this point to eliminate the first derivative in the transformed version of (2.11) by writing

$$\Theta(\eta) = \frac{(1+\beta^2\eta^2)^{1/2}}{(1+\eta^2)^{1/4}} \theta_1(\eta). \quad (2.14)$$

Our new equation is

$$\nu \frac{d^2\Theta}{d\eta^2} + \tilde{Q}_1(\eta)\Theta(\eta) + \frac{1}{\pi} P \int_{-\infty}^{\infty} d\eta' \frac{\tilde{Q}_2(\eta, \eta')\Theta(\eta')}{\eta - \eta'} = \tilde{R}(\eta), \quad (2.15)$$

where

$$\tilde{Q}_1(\eta) = \frac{4\beta^4(1+\eta^2)^{1/2}}{(1+\beta^2\eta^2)^2}, \quad (2.16a)$$

$$\tilde{Q}_2(\eta, \eta') = \frac{4\eta\beta^4(1+\eta^2)^{1/4}(1+\eta'^2)^{1/4}}{(1+\beta^2\eta^2)^{1/2}(1+\beta^2\eta'^2)^{3/2}}, \quad (2.16b)$$

$$\tilde{R}(\eta) = \frac{\eta[3+\beta^2(\eta^2-2)]}{(1+\beta^2\eta^2)^{1/2}(1+\eta^2)^{9/4}}, \quad (2.16c)$$

and

$$\beta = (1+\alpha)^{1/2} = \frac{\lambda}{1-\lambda}. \quad (2.17)$$

Our extension of the range of η to include the negative real axis in (2.15) requires that we consider only symmetric fingers so that θ_1 and Θ are antisymmetric functions of their arguments. Again, in (2.15), we have omitted nonsingular terms of order ν .

In general, the conditions under which an equation of the form (2.15) can be solved are very much more stringent than they are for the related equation in which

the derivative is missing. The mathematical situation is easiest to visualize when one is dealing with a purely local equation, that is, a differential rather than an integral equation. In this case, one can imagine constructing a solution by starting on some special limiting portion of the curve, say, far down one of the sides of the finger, and integrating forward. When the second derivative is present, this procedure is likely to produce completely unacceptable behavior near the tip and on the opposite side of the finger. The reason is that the homogeneous part of the equation has extra solutions which always are rapidly varying and frequently are badly behaved. For example, these extra solutions may diverge at large η . Only under very special circumstances will it be possible to construct a physically sensible particular solution of the inhomogeneous equation in which the badly behaved extra solutions are completely absent. The procedure of actually constructing a particular solution and checking to see whether it is properly behaved has been carried out explicitly for local models of interfacial pattern formation.^{13,14} These calculations have been performed both numerically and analytically, and for both the fully nonlinear and the linearized versions of the local models. It was these investigations in which the solvability mechanism for pattern selection was discovered^{15,16} and which have led us to postulate the existence of a similar mechanism for the nonlocal Saffman-Taylor and dendrite problems.

The mathematical situation looks considerably more difficult when, as in (2.15), the equation also contains a nonlocal term. This integral cannot be assumed to exist at all unless Θ is sufficiently well behaved. We are therefore unhappy with previous discussions, especially our own,⁹ in which it was made to seem as if we were actually constructing a solution for an arbitrary value of ν with, say, a nonzero mismatch angle at the tip or a divergence along one side of the finger. Rather, it seems to us that the best one can do with present analytic techniques is to obtain a necessary but not sufficient condition for the existence of solutions. We shall do this formally by requiring that the inhomogeneous term \tilde{R} on the right-hand side of (2.15) be orthogonal to the null space of the linear operator, say \mathcal{L} , on the left. Even this prescription, however, is an overstatement of what we are actually doing because it implies that we can properly define the function space in which we are working. The true state of affairs is that we can, by WKB methods, compute a null eigenvector Θ_0^\dagger of the adjoint of \mathcal{L} , $\mathcal{L}^\dagger\Theta_0^\dagger=0$, and then write

$$\Lambda(\lambda, \nu) \equiv \int_{-\infty}^{+\infty} d\eta \Theta_0^\dagger \tilde{R} = \int_{-\infty}^{+\infty} d\eta \Theta_0^\dagger \mathcal{L}\Theta = \int_{-\infty}^{+\infty} d\eta \Theta \mathcal{L}^\dagger \Theta_0^\dagger = 0. \quad (2.18)$$

The third equality in (2.18) defines what we mean by the adjoint operator \mathcal{L}^\dagger . This definition makes sense only if Θ_0^\dagger exists and is sufficiently well behaved that all of the integrals in (2.18) are convergent, and if the integration by parts implied at the third step is legal. Finally, existence of the desired solution Θ implies that the solvability function Λ must vanish. But the vanishing of Λ in no way guarantees the existence of Θ .

Only the integral kernel in (2.15) fails to be self-adjoint. Thus, the equation for Θ_0^\dagger is

$$\nu \frac{d^2 \Theta_0^\dagger}{d\eta^2} + \tilde{Q}_1(\eta) \Theta_0^\dagger(\eta) - \frac{1}{\pi} \text{P} \int_{-\infty}^{\infty} d\eta' \frac{\tilde{Q}_2(\eta', \eta) \Theta_0^\dagger(\eta')}{\eta - \eta'} = 0. \quad (2.19)$$

From this point on, our analysis is essentially the same as in Ref. 10, although some of the detailed results are different. We suppose that the solutions of (2.19), say $\Theta_{0\pm}^\dagger(\eta)$, have the WKB form, $\exp[\Psi_\pm(\eta)/\sqrt{\nu}]$, where the $\Psi_\pm(\eta)$ remain finite and smooth in the limit $\nu \rightarrow 0$. Further, we suppose that the $\Psi_\pm(\eta)$ have points of stationary phase $\bar{\eta}_\pm$ in the upper (lower) half of the complex η plane, and that the integral in (2.19) can be evaluated in the limit of small ν by deforming the contour of integration into the path of steepest descent through the appropriate $\bar{\eta}_\pm$. The latter condition requires $\text{Re}\Psi_\pm(\bar{\eta}_\pm) < 0$. Then the only contribution to the integral that is not exponentially small of order $\exp[\Psi_\pm(\bar{\eta}_\pm)/\sqrt{\nu}]$ is the part that comes from integrating around the pole at $\eta = \eta'$. In this way, (2.19) becomes

$$\nu \frac{d^2}{d\eta^2} \Theta_{0\pm}^\dagger + \tilde{Q}_\pm(\eta) \Theta_{0\pm}^\dagger(\eta) = 0, \quad (2.20)$$

where

$$\tilde{Q}_\pm(\eta) = \frac{4\beta^4(1 \pm i\eta)^{3/2}(1 \mp i\eta)^{1/2}}{(1 + \beta^2\eta^2)^2}. \quad (2.21)$$

The WKB solutions of (2.20) are

$$\Theta_{0\pm}^\dagger(\eta) \approx \frac{1}{\tilde{Q}_\pm^{1/4}(\eta)} \exp[\Psi_\pm(\eta)/\sqrt{\nu}], \quad (2.22)$$

where

$$\begin{aligned} \Psi_\pm(\eta) &= \pm i \int_0^\eta d\eta' \tilde{Q}_\pm^{1/2}(\eta') \\ &= \pm 2i\beta^2 \int_0^\eta d\eta' \frac{(1 \pm i\eta')^{3/4}(1 \mp i\eta')^{1/4}}{1 + \beta^2\eta'^2}. \end{aligned} \quad (2.23)$$

The points of stationary phase of $\Theta_{0\pm}^\dagger(\eta)$ occur at $\bar{\eta}_\pm = \pm i$ as required for self-consistency of the above calculation. Note that $\Psi_+(\eta) = \Psi_-^*(\eta)$ and that $\Psi_+(-\eta) = \Psi_-(\eta) = \Psi_+^*(\eta)$; thus the $\Theta_{0\pm}^\dagger(\eta)$ form a complex conjugate pair. Both of the $\Theta_{0\pm}^\dagger(\eta)$ vanish like $|\eta|^{1/2-\sqrt{2}}$ in the limit $|\eta| \rightarrow \infty$, a result which is important in order to assure convergence of the integrations in (2.18). [The null eigenvectors of the original operator \mathcal{L} diverge like $|\eta|^{1/2+\sqrt{2}}$. These power laws are quite different from the exponential behavior found in the dendrite problem. See Eq. (2.20) in Ref. 10.] The antisymmetric combination of the $\Theta_{0\pm}^\dagger$ appropriate for use in the solvability condition (2.18) is

$$\Theta_0^\dagger(\eta) = \frac{1}{2i} [\Theta_{0+}^\dagger(\eta) - \Theta_{0-}^\dagger(\eta)] = \text{Im}\Theta_{0+}^\dagger(\eta). \quad (2.24)$$

Finally, we have

$$\begin{aligned} \Lambda(\lambda, \nu) &= \int_{-\infty}^{+\infty} d\eta \text{Im}\Theta_0^\dagger(\eta) \bar{R}(\eta) \\ &= \frac{1}{i} \int_{-\infty}^{+\infty} d\eta \Theta_{0+}^\dagger(\eta) \bar{R}(\eta) \\ &= \int_{-\infty}^{+\infty} d\eta \bar{F}(\eta) \exp[\Psi_+(\eta)/\sqrt{\nu}] = 0, \end{aligned} \quad (2.25)$$

where

$$\bar{F}(\eta) = -\frac{i\eta[3 + \beta^2(\eta^2 - 2)]}{\sqrt{2}\beta(1 + \eta^2)^{5/2}} \left[\frac{1 - i\eta}{1 + i\eta} \right]^{1/8}. \quad (2.26)$$

In writing (2.25), we have used the antisymmetry of $\bar{R}(\eta)$ and the various symmetries of the $\Theta_{0\pm}^\dagger(\eta)$ deduced above.

In the limit of small ν —the case of physical interest— $\Lambda(\eta, \nu)$ can be evaluated by the method of steepest descent. We have already used the fact that $\Psi_+(\eta)$ has a point of stationary phase at $\eta = \bar{\eta} = +i$ with $\text{Re}\Psi_+(i) < 0$, and we now may expect that the integral in (2.25) will be determined by the behavior of the exponential function in the immediate neighborhood of that point. $\bar{F}(\eta)$ has no singularities on the real axis, therefore we may deform the entire contour of integration into the upper half of the complex η plane. From (2.23), we see that this point of stationary phase is also an algebraic branch point, and that Ψ_+ has an additional nearby logarithmic branch point at $\eta_b = i/\beta$.

Appropriate contours of integration for the evaluation of Λ are shown in Fig. 2 for two qualitatively different situations, $\lambda < \frac{1}{2}$ and $\lambda > \frac{1}{2}$. In the first case, $1/\beta > 1$, and the contour does not pass near η_b . We can perform the integration by expanding Ψ_+ about $\eta = i$:

$$\Psi_+(\eta) \approx -\beta^2 I_0(\lambda) - \frac{8}{7} \left[\frac{2}{i} \right]^{1/4} \left[\frac{\lambda^2}{1 - 2\lambda} \right] (\eta - i)^{7/4}, \quad (2.27)$$

where

$$I_0(\lambda) = 2 \int_0^1 du \frac{(1-u)^{3/4}(1+u)^{1/4}}{1 - \beta^2 u^2}. \quad (2.28)$$

We find

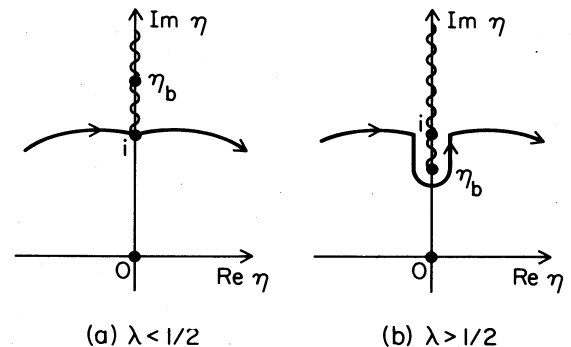


FIG. 2. Contours of integration for evaluating the solvability function Λ .

$$\Lambda(\lambda, \nu) \approx N \frac{\lambda^{6/7}(1-2\lambda)^{1/14}}{(1-\lambda)\nu^{13/28}} \exp \left[-\frac{\beta^2 I_0(\lambda)}{\sqrt{\nu}} \right], \quad (2.29)$$

where $N \simeq 2.008$. From experience with local models,^{13,14} we know that the constant N in formulas of this kind is not determined accurately by the linear theory. The actual value of N is of no importance in the present context but some estimate will be needed later. Equation (2.29) illustrates the singular nature of the capillary perturbation— Λ has no regular series expansion in powers of ν —and also implies the absence of solutions at nonzero ν for $\lambda < \frac{1}{2}$.

For the second case shown in Fig. 2, $\lambda > \frac{1}{2}$, the stationary point $\bar{\eta} = i$ must be interpreted as a complex conjugate pair of points on either side of a branch cut running from $\eta_b = i/\beta$ to $+i\infty$. Accordingly, as shown in the figure, the path of steepest descent must include a section which goes from $\eta = i - \delta$ ($\delta \rightarrow +0$), around the branch point at i/β , and back up to $i + \delta$. If this section of the contour is long enough to contain many oscillations of the integrand, then Λ itself is an oscillating function of its arguments. On the other hand, as λ approaches $\frac{1}{2}$, the branch point comes close enough to the point of stationary phase that the analytic structure is not resolved by the integrand and no oscillations occur in Λ . This analytic mechanism is precisely the same as the one that produces zeros in the solvability function for both local^{13,14} and nonlocal¹⁰⁻¹² models of dendritic solidification. The quantity $\beta^2 - 1$ turns out to be a mathematical analog of the crystalline anisotropy. The general form of Λ as a function of ν for these two different choices of λ is shown schematically in Fig. 3. Note that Λ has infinitely many zeros for $\lambda > \frac{1}{2}$.

The crossover between oscillating and smooth behavior of Λ occurs when the imaginary part of $\Psi_+/\sqrt{\nu}$ changes by an amount of order unity as η moves from one side of the cut to the other at $\bar{\eta} = i$. Integrating (2.23) around the pole at $\eta' = \eta_b = i/\beta$, we find

$$\lim_{\delta \rightarrow 0} [\Psi_+(i+\delta) - \Psi_+(i-\delta)] = 2\pi i \frac{(2\lambda-1)^{3/4}}{(1-\lambda)} \quad (2.30)$$

from which we obtain, for λ near $\frac{1}{2}$,

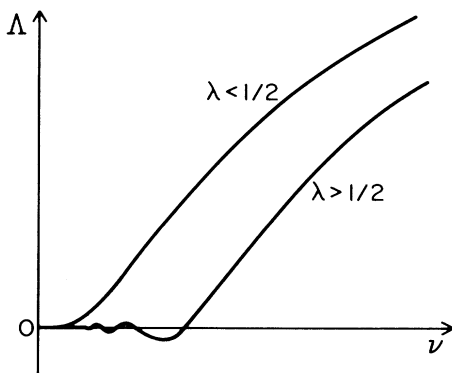


FIG. 3. Qualitative behavior of the solvability function Λ for relative widths $\lambda < \frac{1}{2}$ and $\lambda > \frac{1}{2}$.

$$\lambda - \frac{1}{2} \propto \nu^{2/3}. \quad (2.31)$$

This relationship determines the smallest value of λ at fixed ν or, alternatively, the largest ν at fixed λ for which a steady-state finger exists. Detailed estimates for both the numerical coefficient in (2.31) and the relationship between λ and ν on other branches of the solution have been presented recently by Tanveer.¹⁷ The final step in the argument is to identify the crossover condition (2.31) as the actual selection criterion. As in the case of the dendrites, we argue that the solution with the smallest λ is most likely to be dynamically stable—that broader fingers with flatter fronts would be subject to the same instabilities of the flat surface as those which produced fingers in the first place. We emphasize, however, that none of this analysis touches directly on questions of dynamical stability. (For discussions of the stability of viscous fingers, see Bensimon *et al.*¹⁸ and Kessler and Levine.¹⁹)

III. TIP PERTURBATIONS

Couder and co-workers^{2,3} recently have made an important experimental discovery that graphically illustrates the main features of the solvability mechanism. What they have found is that a small bubble of the inviscid, pushing fluid may become trapped at the tip of a finger and that, when this happens, the properties of the finger are changed in remarkable ways. In particular, the presence of the bubble allows a finger in a channel of width W to have a relative width λ which is appreciably less than $\frac{1}{2}$ and which decreases toward zero as W becomes large.² A related observation pertains to fingers in a radial geometry where, ordinarily, all fingerlike protuberances are unstable against tip splitting because of the absence of sidewalls. When a bubble is trapped on such a finger, the tip stabilizes and moves outward like a dendrite, leaving a train of regularly spaced sidebranches behind it.³

Just how a bubble can become attached to the tip of a finger is not clear at present. The experimental photographs indicate that there is a thin film of the viscous fluid separating the bubble from the finger. (In these experiments, both the finger and the bubble are nitrogen gas, and the viscous fluid into which the finger is being pushed is silicone oil.) The tip of the finger appears to be slightly depressed in a way that somehow must prevent the bubble from falling off to the side. This configuration is sketched schematically in Fig. 4. For our purposes, all that we need to know is that the flow of the viscous fluid is perturbed near the tip. Our proposal is to represent this perturbation in a purely phenomenological way by a nonzero effective opening angle $\Delta\theta$ as shown in the figure. The assumption of a nonzero $\Delta\theta$ has become a familiar mathematical device in numerical formulations of the solvability principle.^{6,20} In general, one can compute shapes of steady-state fingers for arbitrary values of λ and ν if one allows $\Delta\theta$ to be a free parameter. Then the condition that the tip be smooth, $\Delta\theta(\lambda, \nu) = 0$, is a solvability condition. In fact, it must be the same as the solvability condition derived above; that is, $\Delta\theta$ must be proportional to Λ .

One particularly simple way to estimate the relation be-

tween $\Delta\theta$ and Λ within the linear theory is to rewrite (2.15) in the form

$$\nu \frac{d^2\Theta}{d\eta^2} + \tilde{Q}_1(\eta)\Theta(\eta) + \frac{1}{\pi} \mathbf{P} \int_{-\infty}^{\infty} d\eta' \frac{\tilde{Q}_2(\eta, \eta')\Theta(\eta')}{\eta - \eta'} = \tilde{R}(\eta) + \Delta\theta \frac{d}{d\eta} \delta(\eta). \quad (3.1)$$

The new term on the right-hand side containing the derivative of the δ function might be thought of as representing some sort of sharply localized perturbation at the tip of the finger; but the argument for writing this equation is more general. As can be seen by integrating (3.1) twice across an infinitesimally narrow interval including $\eta=0$, the new term amounts simply to a constraint that the first-order correction, $\nu\theta_1$ as defined in (2.10), have a discontinuity of size $\Delta\theta$ at the tip. We argue that, no matter what the actual physical origin of the perturbation, if it is legitimate to deal with it in a linear approximation, then the equation for Θ must have the form shown in (3.1) with, perhaps, $\delta(\eta)$ being replaced by some less sharply localized function of η .

The main uncertainty is how the opening angle $\Delta\theta$ might depend on various parameters like U , W , λ , etc. We shall see that $\Delta\theta$ enters our predictions of experimental results only as the argument of a logarithm. As a result, its precise value is not going to be very important for the simple purpose of demonstrating that a nonzero (positive) $\Delta\theta$ produces fingers with $\lambda < \frac{1}{2}$ in qualitative agreement with experiment. We find it more interesting, however, to try to be a bit more quantitative by examining a suggestion made by Couder *et al.*² Their idea is that the tip of a viscous finger in a sufficiently wide channel might, like the tip of a dendrite, be insensitive to the walls of the system. More specifically, the curvature κ of the tip might be determined only by the flow rate U (via the dimensionless capillary number $\mu U/\gamma$) and not by the channel width W . In what follows, we shall modify their assumption slightly by assuming that it is $\Delta\theta$ rather than

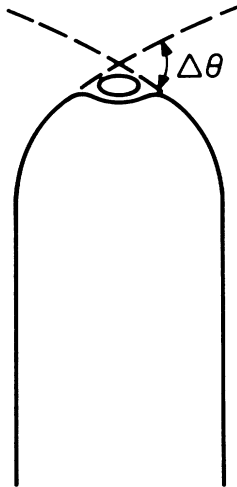


FIG. 4. Schematic illustration of a finger with a bubble trapped at its tip.

κ which depends only on $\mu U/\gamma$. ($\Delta\theta$ might depend also on the ratio of the size of the bubble to the thickness of the cell. However, only a narrow range of bubble sizes is reported to work in the experiments.)

Our next step in the analysis is to multiply (3.1) on the left by $\Theta_0^\dagger(\eta)$ [see (2.24)] and integrate over η . The result is

$$\Lambda(\lambda, \nu) = \Delta\theta \left. \frac{d\Theta_0^\dagger}{d\eta} \right|_{\eta=0} \approx \beta \left[\frac{2}{\nu} \right]^{1/2} \Delta\theta. \quad (3.2)$$

The crucial point is that, for positive values of $\Delta\theta$, we now have a solvability condition that can be satisfied for $\lambda < \frac{1}{2}$. That is, because the right-hand side of (3.2) is positive and nonzero, we can use the upper curve for Λ in Fig. 3 and its analytic approximation in (2.29) to find a new relation between λ and ν for fixed $\Delta\theta$.

There are several useful ways in which to display this relation. The most direct is

$$\Delta\theta \approx N \left(\frac{1}{2} \right)^{1/2} \lambda^{-1/7} (1-2\lambda)^{1/14} \nu^{1/28} \exp \left[- \frac{\beta^2 I_0(\lambda)}{\sqrt{\nu}} \right]. \quad (3.3)$$

Because ν is experimentally of order 10^{-3} and all other parameters entering (3.3) are of order unity, $\Delta\theta$ must be a small angle. It is at this point that the uncertainty in N due to the linear approximation might make some difference; but it should be clear here that our results are going to depend most strongly on the behavior of the exponential term and only relatively weakly on the actual values of $\Delta\theta$ or N .

A second useful form of this relation is obtained by taking the logarithm of both sides of (3.3) and rearranging the ingredients of ν shown in (2.7). The result is

$$\frac{1}{W} = \frac{1}{W_0} \left[\frac{\mu U}{\gamma} \right]^{1/2} \frac{\lambda^2}{(1-\lambda)} I_0(\lambda), \quad (3.4)$$

where the length W_0 is given by

$$W_0 \equiv \frac{\pi b}{(12)^{1/2}} \ln \left[\left[\frac{N}{\Delta\theta} \right] \left[\frac{1}{2} \right]^{1/2} \left[\frac{(1-2\lambda)b}{(1-\lambda)\lambda^2 W} \right]^{1/14} \times \left[\frac{\gamma}{12\mu U} \right]^{1/28} \right]. \quad (3.5)$$

Here we have separated the various terms inside the logarithm in such a way as to emphasize the specially weak dependence of W_0 on all but the first factor, $\Delta\theta/N$, which we assume to depend only on $\mu U/\gamma$. We can now check the consistency of this assumption by computing W_0 from (3.4) using measured values of λ and W at fixed U . A set of four such experimental points (λ, W) , taken from Ref. 2, is shown in Fig. 5 for the case $U=6$ cm/sec. Other relevant parameters are $\gamma=20.9$ dyn/cm, $\mu=0.965$ g/cm sec, and $b=0.1$ cm. All three of the data points for the wider channels, $W=2.0, 3.0,$ and 6.0 cm, yield $W_0 \cong 0.26 \pm 0.01$ cm. For $W=1.0$ cm, we find $W_0 \cong 0.28$ cm. The solid curve in Fig. 5 is a graph of Eq. (3.4) plotted for $W_0 \cong 0.26$ cm. The apparent agreement between

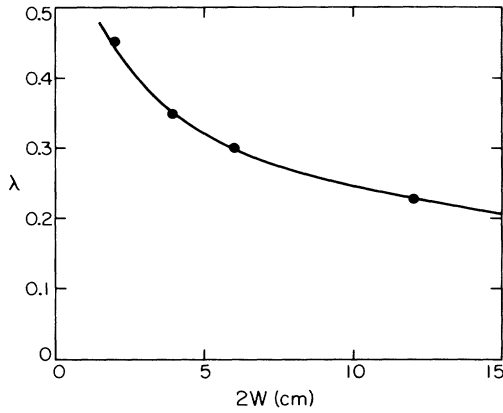


FIG. 5. Relative width λ as a function of the total width of the channel $2W$. The experimental points are those of Couder *et al.* (Ref. 2), and the theoretical curve is a graph of Eq. (3.4) with $W_0=0.26$ cm.

theory and experiment for the W dependence of anomalously small λ 's seems to us to be nontrivial evidence in favor of the proposed selection mechanism.

In order to obtain some information about the U dependence of W_0 and $\Delta\theta$, we have evaluated the above formulas, Eqs. (3.3)–(3.5), using values of λ , W , and U taken from the experimental data displayed graphically in Ref. 2. Our results are shown in Fig. 6 in the form of a graph of $\ln(\Delta\theta)$ as a function of $\mu U/\gamma$. (We have used $N=2.008$ for this purpose.) The width of the shaded region in the figure is a rough measure of our uncertainty which is due, in part, to the scatter in the data but, more importantly, may indicate a breakdown of our assumptions at small W . Note that the values of $\Delta\theta$ deduced in this way decrease from about 0.15 at $\mu U/\gamma=0.1$ to 0.028 at $\mu U/\gamma=0.5$. This downward trend at large velocities

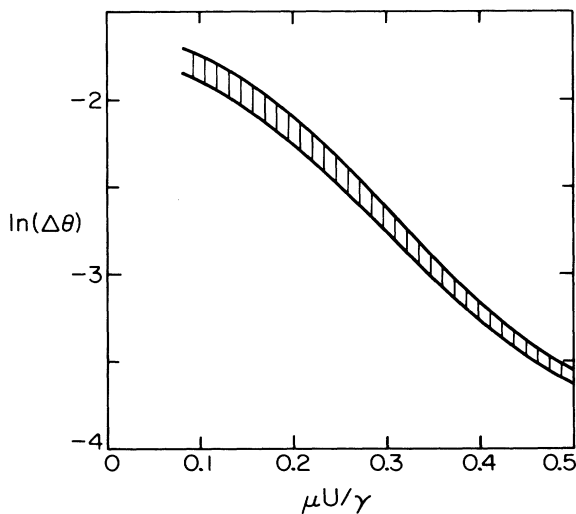


FIG. 6. Estimated variation of $\ln(\Delta\theta)$ as a function of the capillary number ($\mu U/\gamma$) obtained from data in Ref. 2. The experimental points lie roughly within the shaded region.

may have some dynamical significance, but the small size of $\Delta\theta$ argues against the literal interpretation of this quantity as an observable angle.

We return finally to the observation of Couder *et al.* that their graphs of λ versus U for different values of W collapse onto a single curve if they plot, instead of λ , the curvature of the tip of the unperturbed finger as a function of U . That is, they plot

$$\kappa = -\left. \frac{d^2y}{dx^2} \right|_{x=0} = \frac{\pi(1-\lambda)}{2\lambda^2 W}, \quad (3.6)$$

where $y(x)$ is taken from the Saffman-Taylor solution (2.9), and they find (roughly) that κ is a universal function of $\mu U/\gamma$ independent of λ or W . Our theoretical prediction for the right-hand side of (3.6) is

$$\kappa = \frac{\pi}{2W_0} \left[\frac{\mu U}{\gamma} \right]^{1/2} I_0(\lambda). \quad (3.7)$$

This is not precisely the experimental conjecture because the factor I_0 depends, albeit weakly, on λ . However, the experiments reported so far almost certainly were not accurate enough to have detected the λ dependence predicted by (3.7). Graphs of the right-hand side of (3.7) for various values of W do lie within the scatter of the experimental points because, in effect, the U dependence of W_0 has been adjusted to make that happen.

The limit $\lambda \rightarrow 0$ is specially interesting in (3.7) because, according to (3.4), it corresponds to the absence of sidewalls, $W \rightarrow \infty$, and ought therefore to be appropriate for understanding how trapped bubbles produce anomalous dendrite-like fingers in the radial experiments.³ Equation (3.4) implies that the product $\lambda^2 W$ remains finite in the limit $W \rightarrow \infty$. The function $I_0(\lambda)$ is well behaved in this limit: $I_0(0) \cong 1.231$; and the argument of the logarithm defining W_0 in (3.5) is likewise well defined if $\lambda^2 W$ is finite. The similarity to the dendrite theory seems not to be completely precise, however. In the latter theory,^{10–12} the solvability principle determines a special value σ^* of a dimensionless group of parameters, $\sigma \equiv d_0 \kappa^2 D/U$, where d_0 is a capillary length proportional to the surface tension and D is the diffusion constant. As noted above, crystalline anisotropy plays a special role in fixing σ^* . By comparing Eqs. (2.1)–(2.4) to the analogous equations for the dendrite problem, we find that the direct analog of σ for the viscous finger is the group $\bar{\sigma} \equiv \gamma \kappa^2 b^2 / 12 \mu U$. We use (3.7)—and then (3.5)—to obtain

$$\bar{\sigma}^* = \frac{1}{12} \left[\frac{\pi b I_0}{2W_0} \right]^2 \approx \frac{0.379}{[\ln(\Delta\theta)]^2}. \quad (3.8)$$

In the dendrite theory, σ^* is supposed to be independent of U , at least in the limit $U \rightarrow 0$. It is conceivable that the same thing happens to $\bar{\sigma}^*$ in (3.8), but we see no evidence for such an effect. Moreover, we see no reason to believe that theories of pattern selection for these two physically different systems—fingers with bubbles and dendrites with crystalline anisotropy—should be identical at this

level of detail.

In conclusion, the qualitative change in the dynamics of viscous fingers caused by bubbles attached to their tips seems to be a clear demonstration of the general principles of the solvability theory. Positive values of the effective opening angle $\Delta\theta$ produce fingers with relative widths λ less than $\frac{1}{2}$; the further assumption that $\Delta\theta$ depends only on the velocity U leads to quantitatively satisfactory one-parameter comparisons between theory and experiment.

ACKNOWLEDGMENTS

The authors wish to thank Y. Couder and M. Rabaud for showing us their experimental results prior to publication and for useful discussions. This research was supported by U.S. Department of Energy Grant No. DE-FG03-84ER45108 and by National Science Foundation Grant No. PHY-82-17853 supplemented by funds from the U.S. National Aeronautics and Space Administration.

-
- ¹P. G. Saffman and G. I. Taylor, Proc. R. Soc. London, Ser. A **245**, 312 (1958).
²Y. Couder, N. Gérard, and M. Rabaud, Phys. Rev. A **34**, 5175 (1986).
³Y. Couder, O. Cardoso, D. Dupuy, P. Tavernier, and W. Thom, Europhys. Lett. **2**, 437 (1986).
⁴J. S. Langer, Rev. Mod. Phys. **52**, 1 (1980).
⁵J. W. McLean and P. G. Saffman, J. Fluid Mech. **102**, 455 (1981).
⁶J. M. Vanden-Broeck, Phys. Fluids **26**, 2033 (1983).
⁷B. I. Shraiman, Phys. Rev. Lett. **56**, 2028 (1986).
⁸R. Combescot, T. Dombre, V. Hakim, Y. Pomeau, and A. Pumir, Phys. Rev. Lett. **56**, 2036 (1986).
⁹D. C. Hong and J. S. Langer, Phys. Rev. Lett. **56**, 2032 (1986).
¹⁰A. Barbieri, D. C. Hong, and J. S. Langer, Phys. Rev. A **35**, 1802 (1987).
¹¹P. Pelcé and Y. Pomeau, Stud. Appl. Math. **74**, 245 (1986).
¹²M. Ben-Amar and Y. Pomeau, Euro. Lett. **2**, 307 (1986); also, M. Ben-Amar and Y. Pomeau, Physicochemical Hydrodynamics (to be published).
¹³J. S. Langer, Phys. Rev. A **33**, 435 (1986).
¹⁴J. S. Langer and D. C. Hong, Phys. Rev. A **34**, 1462 (1986).
¹⁵R. Brower, D. Kessler, J. Koplik, and H. Levine, Phys. Rev. Lett. **51**, 1111 (1983); Phys. Rev. A **29**, 1335 (1984); D. Kessler, J. Koplik, and H. Levine, *ibid.* **30**, 3161 (1984); **31**, 1712 (1985).
¹⁶E. Ben-Jacob, N. Goldenfeld, J. S. Langer, and G. Schon, Phys. Rev. Lett. **51**, 1930 (1983); Phys. Rev. A **29**, 330 (1984); E. Ben-Jacob, N. Goldenfeld, B. G. Kotliar, and J. S. Langer, Phys. Rev. Lett. **53**, 2110 (1984).
¹⁷S. Tanveer (unpublished).
¹⁸D. Bensimon, L. P. Kadanoff, S. Liang, B. I. Shraiman, and C. Tang, in *Directions in Condensed Matter Physics* (Memorial Volume in honor of Shang-keng Ma), edited by G. Grinstein and G. Mazenko (World Scientific, Singapore, 1986).
¹⁹D. Kessler and H. Levine, Phys. Rev. A **33**, 2621 (1986); **33**, 2634 (1986).
²⁰D. Meiron, Phys. Rev. A **33**, 2704 (1986).